



Arabinose-Induced Catabolite Repression as a Mechanism for Pentose Hierarchy Control in *Clostridium acetobutylicum* ATCC 824

Matthew D. Servinsky,^a Rebecca L. Renberg,^b  Matthew A. Perisin,^a Elliot S. Gerlach,^a Sanchao Liu,^a Christian J. Sund^a

^aU.S. Army Research Laboratory, RDRL-SEE-B, Adelphi, Maryland, USA

^bGeneral Technical Services, Adelphi, Maryland, USA

ABSTRACT Bacterial fermentation of carbohydrates from sustainable lignocellulosic biomass into commodity chemicals by the anaerobic bacterium *Clostridium acetobutylicum* is a promising alternative source to fossil fuel-derived chemicals. Recently, it was demonstrated that xylose is not appreciably fermented in the presence of arabinose, revealing a hierarchy of pentose utilization in this organism (L. Aristilde, I. A. Lewis, J. O. Park, and J. D. Rabinowitz, *Appl Environ Microbiol* 81:1452–1462, 2015, <https://doi.org/10.1128/AEM.03199-14>). The goal of the current study is to characterize the transcriptional regulation that occurs and perhaps drives this pentose hierarchy. Carbohydrate consumption rates showed that arabinose, like glucose, actively represses xylose utilization in cultures fermenting xylose. Further, arabinose addition to xylose cultures led to increased acetate-to-butyrate ratios, which indicated a transition of pentose catabolism from the pentose phosphate pathway to the phosphoketolase pathway. Transcriptome sequencing (RNA-Seq) confirmed that arabinose addition to cells actively growing on xylose resulted in increased phosphoketolase (CA_C1343) mRNA levels, providing additional evidence that arabinose induces this metabolic switch. A significant overlap in differentially regulated genes after addition of arabinose or glucose suggested a common regulation mechanism. A putative open reading frame (ORF) encoding a potential catabolite repression phosphocarrier histidine protein (Crh) was identified that likely participates in the observed transcriptional regulation. These results substantiate the claim that arabinose is utilized preferentially over xylose in *C. acetobutylicum* and suggest that arabinose can activate carbon catabolite repression via Crh. Furthermore, they provide valuable insights into potential mechanisms for altering pentose utilization to modulate fermentation products for chemical production.

IMPORTANCE *Clostridium acetobutylicum* can ferment a wide variety of carbohydrates to the commodity chemicals acetone, butanol, and ethanol. Recent advances in genetic engineering have expanded the chemical production repertoire of *C. acetobutylicum* using synthetic biology. Due to its natural properties and genetic engineering potential, this organism is a promising candidate for converting biomass-derived feedstocks containing carbohydrate mixtures to commodity chemicals via natural or engineered pathways. Understanding how this organism regulates its metabolism during growth on carbohydrate mixtures is imperative to enable control of synthetic gene circuits in order to optimize chemical production. The work presented here unveils a novel mechanism via transcriptional regulation by a predicted Crh that controls the hierarchy of carbohydrate utilization and is essential for guiding robust genetic engineering strategies for chemical production.

KEYWORDS *Clostridium acetobutylicum*, RNA-Seq, biofuel, carbohydrate metabolism, Crh, pentose, phosphoketolase, transcriptional regulation


Received 15 May 2018 Accepted 13 September 2018 Published 23 October 2018

Citation Servinsky MD, Renberg RL, Perisin MA, Gerlach ES, Liu S, Sund CJ. 2018. Arabinose-induced catabolite repression as a mechanism for pentose hierarchy control in *Clostridium acetobutylicum* ATCC 824. *mSystems* 3:e00064-18. <https://doi.org/10.1128/mSystems.00064-18>.

Editor Jeff Tabor, Rice University

This is a work of the U.S. Government and is not subject to copyright protection in the United States. Foreign copyrights may apply.

Address correspondence to Matthew D. Servinsky, matthew.d.servinsky.civ@mail.mil, or Christian J. Sund, christian.j.sund.civ@mail.mil.

 Arabinose-induced catabolite repression as a mechanism for pentose hierarchy control in *Clostridium acetobutylicum* ATCC 824

The genus *Clostridium* is composed of Gram-positive, spore-forming, obligate anaerobic bacteria. While proteolytic species such as *Clostridium perfringens*, *Clostridium difficile*, *Clostridium tetani*, and *Clostridium botulinum* are human pathogens, many are harmless saccharolytic residents of animal intestines and soil (1). These organisms play a vital role in the carbon cycle through fermentation of the carbohydrates found in biomass. The capacity of solventogenic clostridia to convert carbohydrates to valuable solvents and hydrogen gas has long been commercially harnessed in a process known as acetone-butanol-ethanol (ABE) fermentation. ABE fermentations have traditionally employed expensive food-based feedstocks, which made the process economically unfavorable compared to petroleum-based production (2). Rising costs of petroleum and global food shortages have led to increased interest in fermentation of lignocellulosic biomass, such as switch grass and elephant grass, as well as waste plant matter from agricultural and lumber industries (i.e., wheat straw, corn stover, and sawdust) (3).

Lignocellulosic biomass is the most abundant renewable resource for biofuel production, is widely available at low cost, is generally not utilized, and can contain up to 70 to 80% (wt/wt) carbohydrates that can be readily utilized for fermentation (4, 5). After acid pretreatment and enzymatic hydrolysis of polysaccharides to soluble sugars, the weight/weight sugar composition of wheat straw, a representative lignocellulosic biomass, is 56% D-glucose, 38% D-xylose, and 4% L-arabinose (6). Due to the sugar composition of lignocellulosic biomass and the historical use of clostridia in ABE fermentations, there has been great interest in investigating how the organism utilizes xylose and arabinose in the presence of glucose (7, 8). A greater understanding of these control mechanisms will potentially enable full, simultaneous utilization of hexoses and pentoses from lignocellulosic biomass and allow for fine-tuning of preferred end products. A schematic of the currently understood utilization pathways for these pentose sugars is depicted in Fig. 1A (9–14). Arabinose and xylose are thought to be transported into the cell by sugar cation symporters with the catabolic pathways for the two pentoses converging at xylulose-5-P.

The phosphoketolase pathway (PKP) was characterized in our lab and independently by Liu et al. and was shown to be important during pentose metabolism (15, 16) (Fig. 1A). The PKP requires a single enzyme, phosphoketolase (CA_C1343). In *Clostridium acetobutylicum*, the phosphoketolase is bifunctional, cleaving xylulose-5-P to glyceraldehyde-3-P and acetyl-P, as well as fructose-6-P to erythrose-4-P and acetyl-P (15, 16). Recent studies have investigated the roles of the pentose phosphate pathway (PPP) and the PKP during fermentation of xylose and arabinose individually, as well as in cofermentations of the two pentose sugars (15–18). Microarray analysis revealed significantly higher levels of phosphoketolase (CA_C1343) mRNA in cells grown on arabinose compared with glucose (19.4-fold) or xylose (6.7-fold), suggesting that flow through the PKP increases when cells are grown with arabinose as the carbon source compared to glucose or xylose (15, 19). The flux of arabinose through the PKP has been quantified using ¹³C flux and confirms that the cells favor the PKP during growth on arabinose (16–18). Aristilde et al. also observed that *C. acetobutylicum*, like *Escherichia coli*, has a preference for arabinose over xylose (17). In addition, Liu et al. and Sund et al. discovered that catabolic flux through the PKP in *C. acetobutylicum* can be increased with higher xylose concentrations (16, 18). Recent metabolic flux analyses corroborate our previous findings that arabinose is metabolized via the PKP to a greater extent than xylose when grown on similar substrate concentrations (17, 18).

C. acetobutylicum, when grown on a mixture of sugars, will utilize the preferred sugar(s) before consuming any other sugars present, as is the case for many bacteria (5). This process of preferred sugar consumption is known as carbon catabolite repression (CCR) (20). Glucose and mannose are favored by *C. acetobutylicum*, and their dominance over xylose and arabinose is well characterized (21). In Gram-positive bacteria, glucose-mediated CCR is governed by the phosphoenolpyruvate-dependent phosphotransferase system (PTS) and the catabolite control protein A (CcpA), which binds catabolite-responsive elements (CRE) in the genome (20). Phosphorylation of phosphocarrier histidine protein (HPr) at a C-terminal serine by HPr kinase results in HPr-S-P, which then

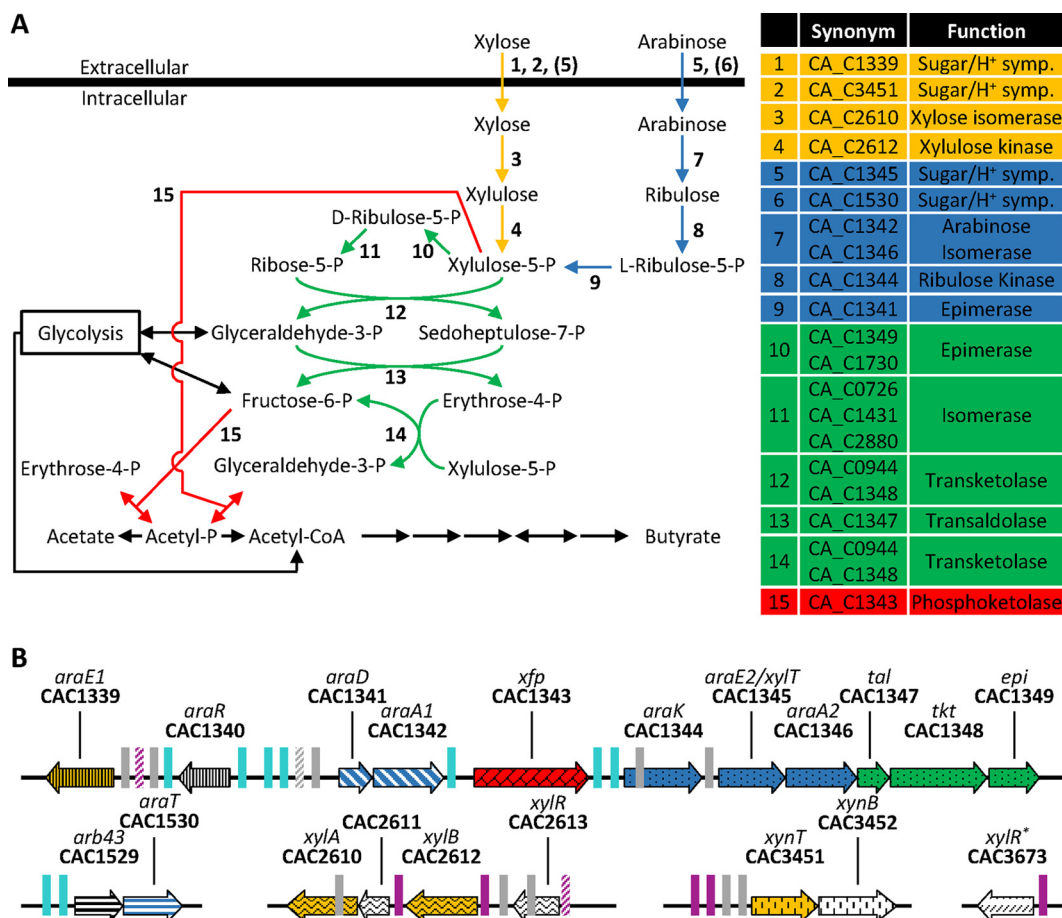


FIG 1 Schematic of pentose catabolism and the genomic structure of the involved genes. (A) Arabinose and xylose metabolism via the pentose phosphate pathway (PPP) (green arrows) and the phosphoketolase pathway (PKP) (red arrows). (B) Map of arabinose and xylose metabolism-associated genes: xylose associated (yellow arrows), arabinose associated (blue arrows), PPP genes (green arrows), and phosphoketolase (red arrow). The pattern within each arrow illustrates operon grouping. Turquoise bars indicate AraR binding sites, purple bars indicate XylR binding sites, and gray bars indicate CcpA binding sites (CRE). Striped bars indicate color-respective repressor sites proposed in this article. Asterisk indicates gene previously identified as an XylR, but most likely incorrectly annotated. Data from references 9, 10, 23, and 28 were used and expanded upon to construct these schematics.

binds to CcpA, generating the functional repressive complex (22). Catabolite regulation by CcpA has been characterized in *C. acetobutylicum*, and genes encoding HPr and HPr kinase are present in the genome (23, 24). In some other Gram-positive bacteria, a second protein Crh (catabolite repression HPr) can be phosphorylated by HPr kinase and activate CcpA (25). In contrast to CcpA, Crh proteins cannot phosphorylate enzyme I of the PTS because of a glutamine residue present at the N-terminal histidine phosphorylation site that is required for PTS phosphorylation (26). CRE sites are found within the promoter or coding sequence of operons for nonpreferred carbohydrates and allow PTS-mediated inhibition of their transcription (27). CcpA binding sites in the *C. acetobutylicum* genome have been identified computationally both within and upstream of coding regions for xylose and arabinose metabolic genes using the *Bacillus subtilis* CRE consensus sequence as well as by electrophoretic mobility shift assay (EMSA) (23, 28). *C. acetobutylicum* transcriptional profiles confirm that genes with predicted CcpA binding sites are significantly repressed in the presence of glucose (14, 19). It is unknown if pentose metabolism in *C. acetobutylicum* can generate similar regulation.

In *C. acetobutylicum*, pentoses are thought to be transported via proton symporters and therefore are not expected to interact with components of the PTS (29). The regulators of xylose and arabinose catabolic genes, XylR and AraR, respectively, act as

repressors of transcription in *C. acetobutylicum* (9, 30). Although two proteins have been proposed to perform the function of the xylose repressor XylR (CA_C3673 and CA_C2613), it is most likely that CA_C2613 is the primary xylose repressor based on experimental findings and data presented here (10, 28, 30). XylR binding sites have been identified both computationally and experimentally upstream and within the predicted CA_C2612-CA_C2611-CA_C2610 operon and computationally for the CA_C3451-CA_C3452 operon (10, 28). Elevated transcript levels for these genes have been recorded for cells grown on xylose compared to those grown on arabinose or glucose, suggesting that the predicted XylR and CRE sites are functional (14, 19). Rodionov et al. identified AraR (CA_C1340) binding sites upstream of CA_C1339, CA_C1340, the predicted CA_C1341-CA_C1342 operon, CA_C1343, the predicted CA_C1344-CA_C1349 operon, and the predicted CA_C1529-CA_C1530 operon (28). The binding of AraR to these sites was confirmed by EMSA, and mRNA levels of these genes were found to be higher in cells grown on arabinose than in xylose or glucose cultures (9). One notable exception is CA_C1339, a proposed xylose importer gene, which has a unique transcription profile with high mRNA levels in cells grown on xylose, moderate levels for those on arabinose, and extremely low levels on glucose (Fig. 1B) (9, 14, 19, 28).

Pentose metabolism has been studied extensively in *E. coli*, a Gram-negative bacterium, where arabinose has been shown to be preferentially utilized over xylose (31–34); however, this phenomenon has not been extensively explored in Gram-positive bacteria. We previously observed a significant disparity in the growth rate of *C. acetobutylicum* ATCC 824 when fermenting arabinose compared to xylose, with xylose-fermenting cultures growing significantly slower and having a substantially longer lag phase (19). This extended lag phase was also observed in Fig. S5 in the supplemental material from Aristilde et al. (17), in which the carbohydrate was almost completely consumed in an arabinose-fed culture before the culture fed with xylose began to appreciably utilize the sugar (17). Additionally, Aristilde used ^{13}C flux analysis to show that there was a preference for arabinose over xylose when the organism was provided both pentoses simultaneously (21).

Although the preferential utilization of arabinose over xylose in *C. acetobutylicum* has been documented, the mechanism (or mechanisms) driving this preference is not known. A better understanding of the mechanism behind the preferential use of arabinose over xylose would be beneficial in order to identify methods to fully utilize all the fermentable sugars present in readily available lignocellulosic biomass. We hypothesized that active repression of xylose utilization via transcriptional control will occur in the presence of arabinose. To test this hypothesis, we examined the effects of addition of glucose, arabinose, or xylose independently to *C. acetobutylicum* cultures actively growing on xylose. In addition to performing transcriptome sequencing (RNA-Seq) at various time points after addition of supplemental sugar, we examined growth, accumulation of organic end products, and carbohydrate utilization.

RESULTS

(i) Growth. *C. acetobutylicum* ATCC 824 was grown on xylose with different carbohydrate supplementations during early exponential growth to measure the effects of such additions. Noticeable effects on the cultures' growth profiles at the beginning of the exponential growth phase were observed when the cultures were initially grown on 0.5% xylose and subsequently supplemented with 0.25% arabinose [(+)Ara], 0.25% glucose [(+)Glu], 0.25% xylose [(+)Xyl], or no additional sugar [(+)None] as shown in Fig. 2A. (+)None and (+)Xyl cultures had similar doubling times, and addition of xylose extended exponential growth in (+)Xyl by approximately 2 h beyond that seen in (+)None. The growth rates in the (+)Ara cultures were significantly increased over the other three culture conditions and reached their maximum doubling time by the 2nd hour after sugar supplementation, whereas the (+)Glu cultures did not reach their maximum doubling time until between hours 3 and 5 (Fig. 2A).

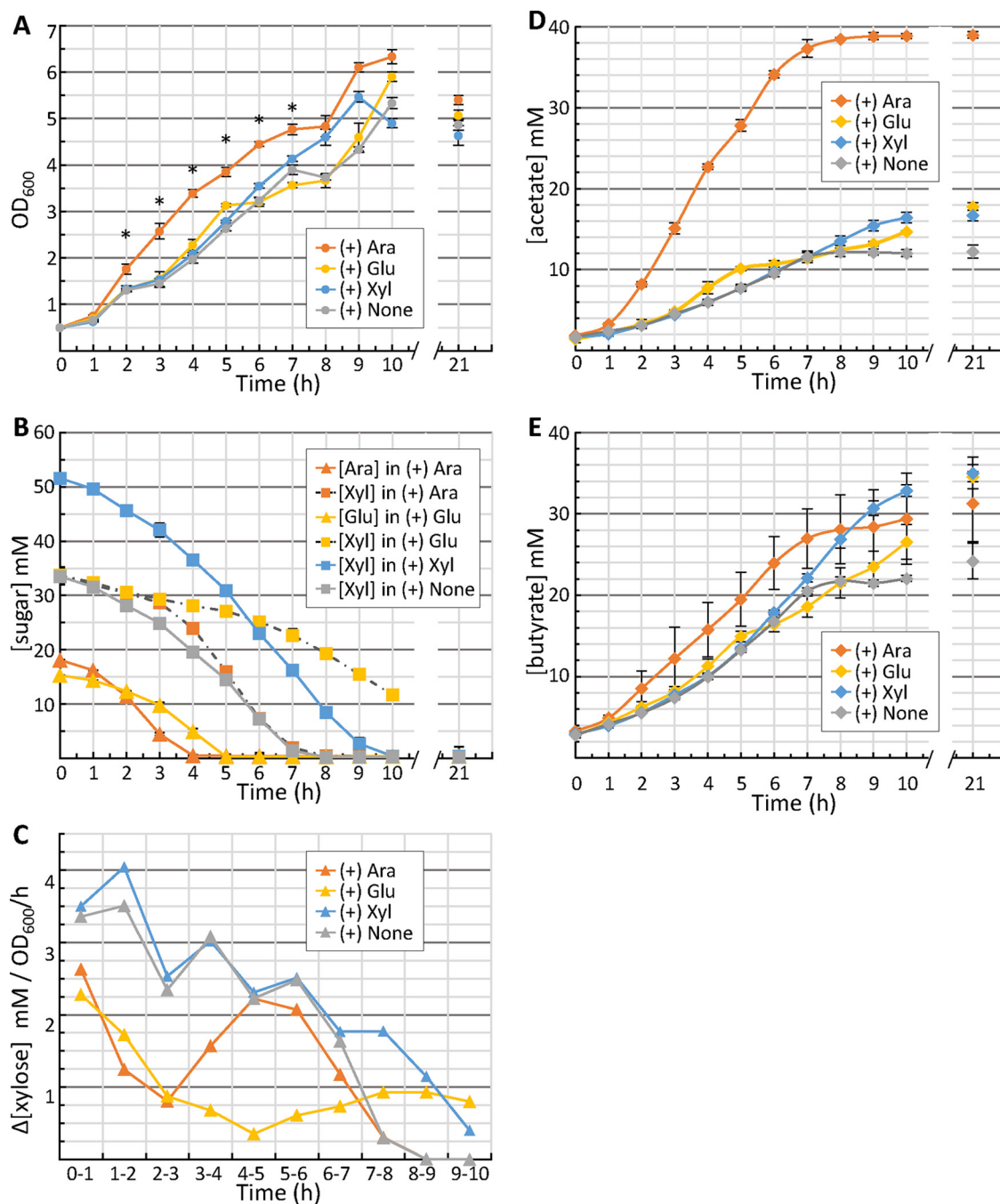


FIG 2 Arabinose supplementation alters growth rate, global sugar consumption, and acid production in *C. acetobutylicum*. (A) Growth curves of cultures after supplemental sugar addition. Error bars are standard deviations. * indicates two-tailed Student's *t* test <0.01 for (+)Ara compared to (+)Glu, (+)Xyl, or (+)None. (B) Global sugar consumption in each culture was monitored after supplemental sugar addition by quantifying the amount of each sugar in the medium at each time point. Error bars are standard deviations. (C) Change in xylose concentration normalized to average OD_{600} for each hour after supplemental sugar addition. (D) Acetate concentrations in culture medium were monitored every hour after supplemental sugar addition, and reported values are the average from all experiments. (E) Butyrate concentrations in culture medium were monitored every hour after supplemental sugar addition, and reported values are the average from all experiments.

(ii) Sugar consumption. Addition of xylose increased the amount of time that it took (+)Xyl to be completely depleted of xylose compared to (+)None, which was expected (Fig. 2B). The (+)Ara depleted arabinose and xylose in the medium after approximately 4 h and 8 h, respectively, while (+)Glu depleted glucose from the medium after 5 h and still had greater than 25% of the initial xylose after 10 h of fermentation (Fig. 2B).

Since there were differences in growth rates between the cultures on the various sugars, we normalized xylose consumption based on optical density at 600 nm (OD_{600}) and expressed it as the change in xylose concentration per the average OD_{600} (average of OD_{600} at beginning and end of time corresponding to ΔmM measurements) per hour designated $\Delta mM/OD_{600(avg)}/h$ (Fig. 2C). Xylose in (+)None and (+)Xyl was depleted initially at a rate of between 3.0 and 4.0 $\Delta mM/OD_{600(avg)}/h$ during the first 2 h postaddition and stayed above 2.0 $\Delta mM/OD_{600(avg)}/h$ through most of the exponential growth phase. Xylose consumption in (+)Glu was dramatically slowed, dropping to below 1.0 $\Delta mM/OD_{600(avg)}/h$ by hour 3 and reaching 0.36 $\Delta mM/OD_{600(avg)}/h$ at hour 5, at which point the glucose was exhausted from the medium. Xylose consumption in (+)Ara was even lower than was observed in (+)Glu after 2 h [1.24 versus 1.72 $\Delta mM/OD_{600(avg)}/h$] and equivalent to it after 3 h [0.87 $\Delta mM/OD_{600(avg)}/h$]. Once arabinose was depleted at hour 4, the rate of xylose consumption matched that seen in (+)None (Fig. 2C).

(iii) Metabolic output. Both xylose and arabinose are known to be metabolized through the PPP (which favors butyrate production) and PKP (which favors acetate production), and the relative flux through the two pathways is reflected in the ratio and concentration of acetate and butyrate produced (17). Compared to the PPP, the PKP oxidizes a lower proportion of carbon to CO_2 , which is coupled to a decrease in the reduction of the electron carriers NAD^+ and ferredoxin. The decreased reduction of NAD^+ to $NADH$ in the PKP lessens the need to use acetyl coenzyme A (acetyl-CoA) as an electron acceptor to reoxidize $NADH$ to NAD^+ through butyrate formation. This allows the cells to use acetyl-CoA for ATP formation via conversion to acetate, which yields 1 ATP/acetyl-CoA, compared to butyrate formation, which yields 0.5 ATP/acetyl-CoA (18). Final concentrations of acetate (Fig. 2D) and butyrate (Fig. 2E) were measured in order to infer the influence that sugar addition may have on relative flux through the PPP and PKP. The final (+)None and (+)Xyl acetate-to-butyrate ratios were similar, 0.51 ± 0.06 and 0.48 ± 0.03 , respectively. Glucose addition resulted in a two-phase production of acetate and butyrate and had a final ratio of 0.51 ± 0.02 , which is comparable to the (+)None and (+)Xyl. Compared to the other cultures, (+)Ara had much higher concentrations of acetate, 39 ± 0.4 mM, but similar final concentrations of butyrate, resulting in a final acetate-to-butyrate ratio of 1.3 ± 0.2 .

(iv) Transcriptional analysis. To measure transcriptional responses to sugar supplementation of cultures actively growing on xylose, transcriptome sequencing (RNA-Seq) was performed for each condition over a 60-min time period after supplemental sugar addition. RPKM (Reads Per Kilobase of transcript per Million mapped reads) values were calculated, and genes that met the statistical cutoffs described in Materials and Methods were examined further. Hierarchical clustering of Euclidean distances for samples and genes was performed on the filtered gene set, and the results are presented in Fig. 3A. (+)Ara 15- and 30-min samples clustered most closely to the preaddition samples, and (+)Ara 60 min clustered most closely with the (+)Glu (15-, 30-, and 60-min) samples, with (+)Glu 60 min clustering closest to (+)Ara 60 min. Further analysis of the differentially expressed genes indicated that 190 and 278 genes had altered mRNA expression levels after addition of arabinose and glucose, respectively. Of the differentially expressed genes, 146 were common between arabinose and glucose addition and 89 of these genes have been shown to be controlled by CcpA (23) (Fig. 3B). Gene clustering showed that genes controlled by CcpA and AraR or XylR were clustered together, but CcpA-controlled genes that lacked AraR or XylR control did not show a distinct clustering pattern (Fig. 3A, columns on right-hand side). Two notable genes are *xfp* (CA_C1343) and CA_C0149, which did not cluster closely with other differentially expressed genes. Phosphoketolase is encoded by *xfp*, and this gene differs from other AraR-controlled genes because it appears to lack a CRE site. CA_C0149, which has a predicted CRE site, was the most differentially regulated gene, with mean RPKM values of 69,182 and 61,658 for (+)Glu and (+)Ara preaddition samples, respec-

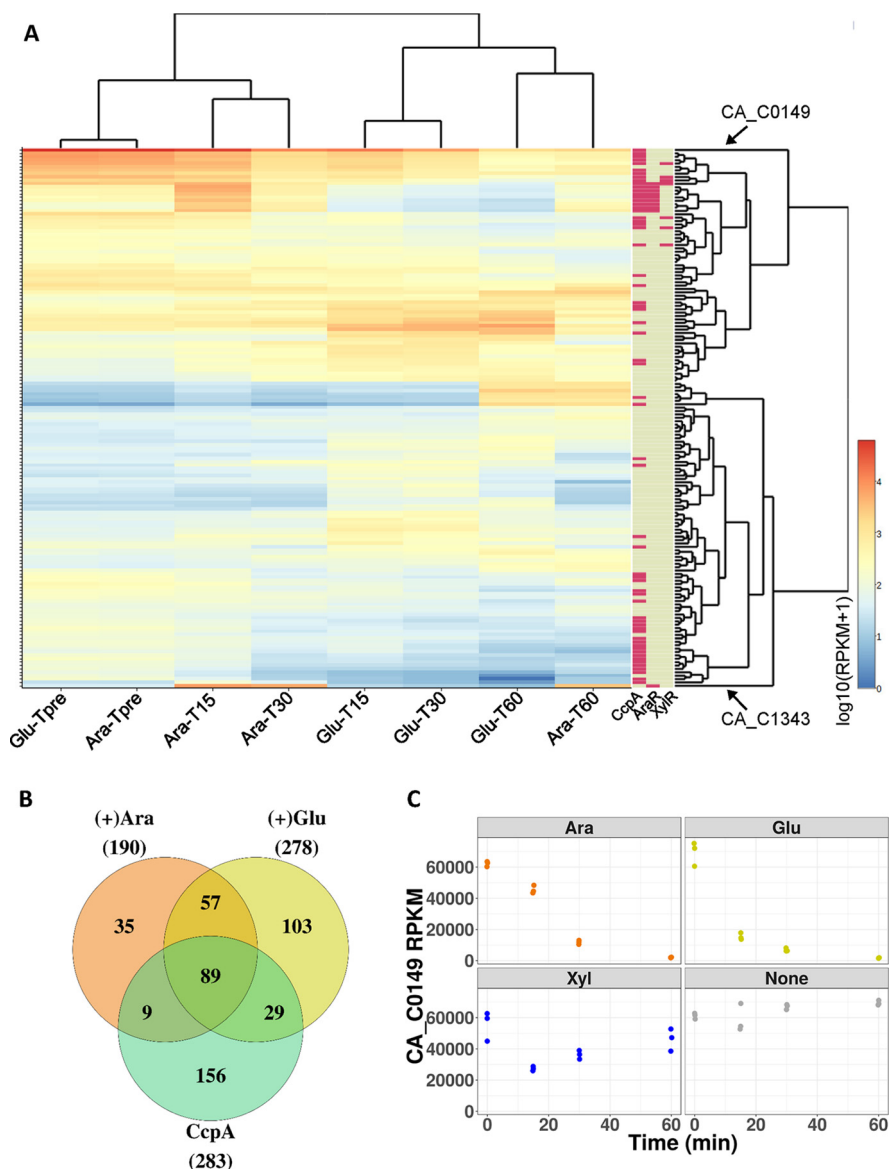


FIG 3 Comparison of differentially expressed genes. (A) Cultures actively growing on xylose were supplemented with an additional sugar (glucose or arabinose), and samples were taken for RNA-Seq at 15, 30, and 60 min after supplementation. Heat map and hierarchical clustering results of differentially regulated genes from RNA-Seq samples. The columns on the right indicate the presence of CcpA, AraR, or XylR binding sites in coding or promoter regions of the genes. CA_C0149 (hypothetical) and CA_C1343 (*xfp*) are noted. Samples on the x axis are labeled by the supplemental sugar and the time point (i.e., Glu-T15 = glucose supplementation culture 15 min after supplemental sugar addition). (B) Venn diagram showing overlap between genes differentially regulated after arabinose addition or glucose addition with genes containing CcpA binding sites at 60 min after supplemental sugar addition. (C) Temporal response of CA_C0149 after addition of supplemental sugars. Each point represents a biological replicate. The x axis marks time after carbohydrate supplementation, and the y axis marks the CA_C0149 expression level in terms of reads per kilobase of transcript per million mapped reads (RPKM). Each panel displays results for each different carbohydrate supplementation: glucose (Glu), arabinose (Ara), xylose (Xyl), or no carbohydrate (None).

tively, and 1,697 and 2,040 in the (+)Glu 60 min and (+)Ara 60 min samples, respectively (Fig. 3C).

All of the differentially expressed genes were divided into groups based on the presence and/or absence of a CcpA, AraR, and XylR binding site (predicted and known; see Materials and Methods), and the \log_2 fold change (compared to preaddition samples) of these genes was plotted for all time points to capture the temporal

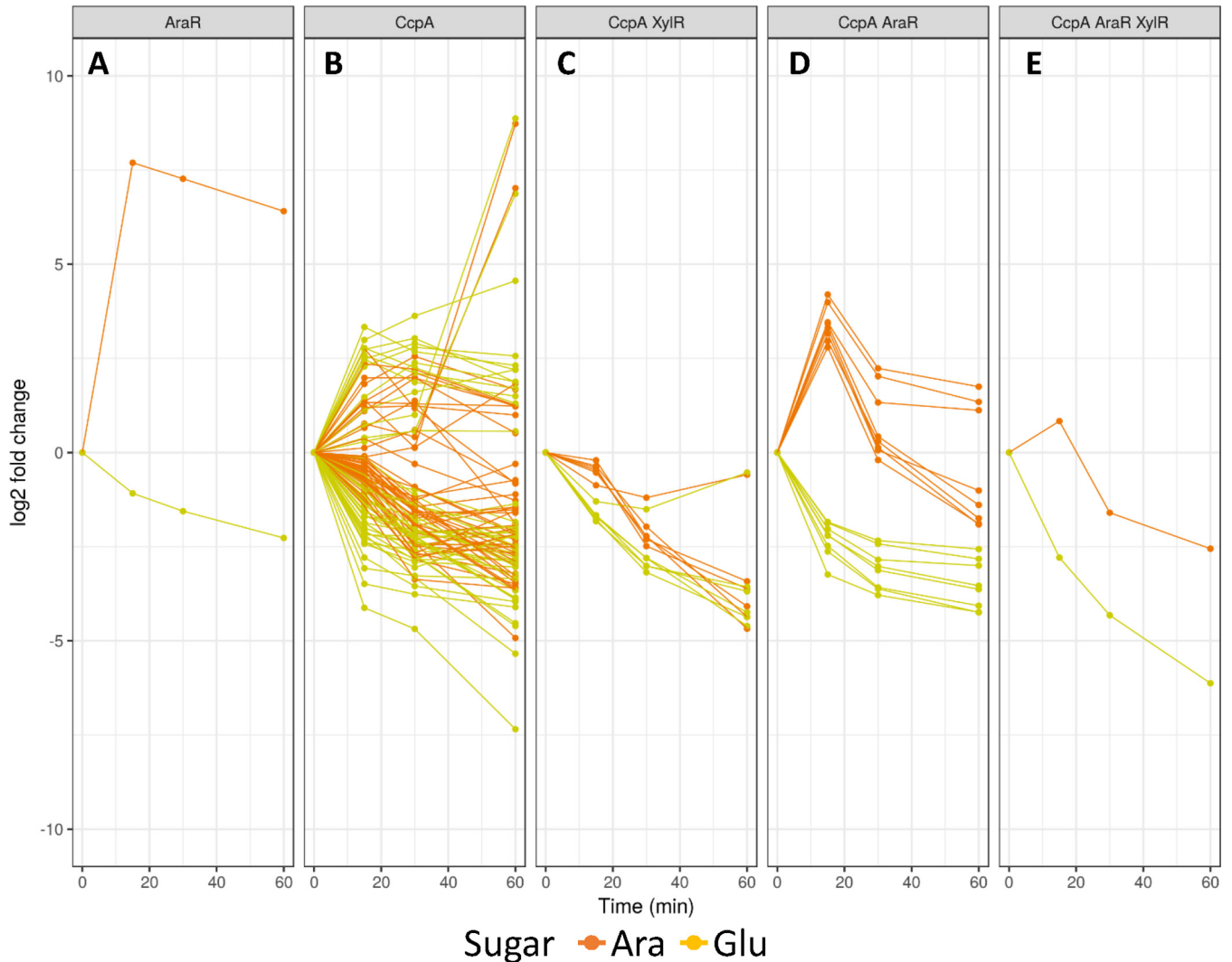


FIG 4 Temporal response of differentially expressed genes after addition of glucose or arabinose expressed as log₂ of fold change relative to preaddition levels. (A) Genes with identified AraR sites but lacking XylR and CcpA sites. (B) Genes with CcpA binding sites, but not AraR or XylR binding sites. (C) Genes with identified CcpA and XylR sites but lacking AraR binding sites. (D) Genes with identified CcpA and AraR binding sites but lacking identified XylR sites. (E) Genes with identified CcpA, AraR, and XylR binding sites. Each line represents a single gene, and the color of the line corresponds to the supplemental sugar added. The other two possibilities, AraR/XylR and XylR, contained no differentially expressed genes and were not represented in this figure.

response to sugar addition (Fig. 4). For (+)Xyl and (+)None, there was very little change in expression over the course of the experiment, regardless of presence or absence of CcpA, AraR, or XylR binding sites (see Fig. S1 in the supplemental material). There were many genes without known or predicted CcpA, AraR, or XylR binding sites that were differentially expressed in response to glucose and/or arabinose addition. We removed these genes from further analysis to focus on differential expression due to the interplay of known transcription factors. There was a single differentially expressed gene, CA_C1343 (*xfp*), with an AraR binding site and lacking CcpA and XylR binding sites that showed substantial changes in expression levels upon addition of arabinose (Fig. 4A, orange line) and glucose (Fig. 4A, yellow line). Differentially expressed genes with a CcpA binding site, but lacking AraR and XylR binding sites, showed significant changes in expression upon the addition of glucose, as expected (Fig. 4B, yellow lines), and many of these genes were also modulated by the addition of arabinose; however, the response to arabinose addition was delayed in some cases (Fig. 4B, orange lines). Differentially expressed genes with CcpA and XylR binding sites and lacking an AraR binding site showed decreased expression over time upon addition of glucose (Fig. 4C,

yellow lines) and arabinose (Fig. 4C, orange lines). Differentially expressed genes with CcpA and AraR binding sites but lacking a XylR binding site were initially induced by the addition of arabinose, but expression levels returned to near preaddition levels by the 60-min time point (Fig. 4D, orange lines), whereas the expression of all of these genes was repressed upon addition of glucose (Fig. 4D, yellow lines). The final group analyzed were those differentially expressed genes with CcpA, AraR, and XylR binding sites (Fig. 4E). A single differentially expressed gene, CA_C1339, with all three binding sites had reduced expression upon addition of glucose and arabinose, with a notable delay in response to arabinose addition. The two other potential combinations of the binding sites, CcpA(-)/AraR(+)/XylR(+) and CcpA(-)/AraR(-)/XylR(+), did not have any genes that met the criteria for differential gene expression and consequently were not included in this figure.

(v) Putative catabolite repression HPr (Crh). CA_C0149, encoding a putative Crh of *C. acetobutylicum*, was the most differentially regulated gene upon addition of glucose or arabinose (Fig. 3C). This gene was repressed in the presence of both sugars, with a delayed response noticeable with addition of arabinose. Alignment of the CA_C0149-derived amino acid sequence with Crh sequences from several *Bacillus* species (Fig. 5A) shows similarity between these proteins. In the alignment, the CA_C0149-encoded protein has a glutamine residue at position 26, which aligns with the glutamine residues of the other Crh sequences and the histidine of the putative HPr of *C. acetobutylicum* at the same position. This glutamine residue is a key difference between Crh and HPr, as the histidine at this position is required for the HPr-mediated phosphate transfer to the PTS (26). In addition, the CA_C0149-derived sequence contains a serine at position 54, which aligns with serine residues of other Crh sequences and the putative HPr of *C. acetobutylicum*. HPr kinase phosphorylates this serine residue, thereby activating HPr/Crh, in turn leading to CcpA-mediated catabolite repression in other organisms. Transcriptional levels of CA_C0149 during growth on 11 different carbohydrates were obtained from a previous study and show that expression levels are higher during growth on less preferred carbohydrates (Fig. 5B) (19).

DISCUSSION

It has been demonstrated that *C. acetobutylicum* has a hierarchy of pentose utilization, with arabinose being utilized preferentially to xylose when both sugars are present at the beginning of the fermentation (17). This hierarchy could be due to inherent differences in growth rates on the two pentoses as there is an extremely long lag phase in *C. acetobutylicum* fermentations of xylose compared to arabinose, but there may be other levels of regulation that play a role in arabinose preference. To further the understanding of this pentose hierarchy, we monitored exponential-growth-phase cultures utilizing xylose that were supplemented with one of the following sugars: arabinose, glucose, or xylose. Measurements of growth, sugar utilization, and mRNA transcript levels revealed that, as with glucose, addition of arabinose inhibits xylose utilization and modulates transcription of xylose utilization genes and other CcpA-controlled genes. Additionally, increased acetate/butyrate ratios after arabinose addition indicated that pentose metabolism likely shifted from the PPP to the PKP.

Previous studies showed that growth on glucose and arabinose is faster than on xylose, and the experiments shown here confirm and expand upon that knowledge (19). When arabinose was added to a xylose fermentation, the arabinose was rapidly utilized and the growth rate increased. Glucose addition had a different effect, instead maintaining growth comparable to control in the first 2 h with an increased growth rate between hours 3 and 5 (Fig. 2A). This is counterintuitive to what was expected given the growth rates on glucose or arabinose alone. The difference in the time to utilize the two preferred carbohydrates could be due to the metabolic state of the cells upon addition of arabinose or glucose. The machinery for glucose utilization is present and only needs to be activated, which upon glucose addition could lead to a rapid influx of glycolytic intermediates or generation of toxic by-products such as methylglyoxal, both of which have been shown to inhibit metabolism (35, 36). In contrast, when arabinose

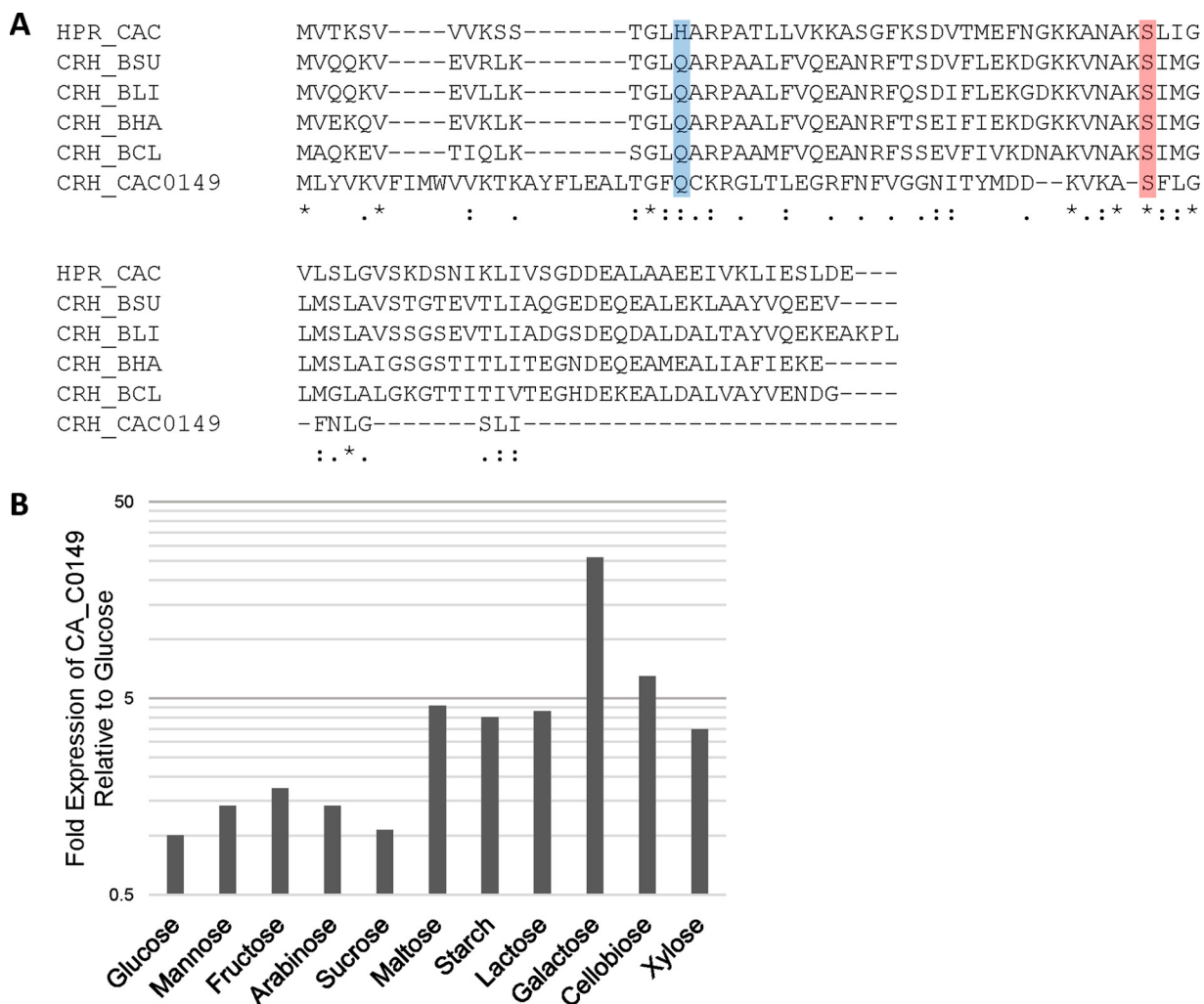


FIG 5 Putative Crh (CA_C0149) alignment and mRNA expression levels. (A) Alignment of *C. acetobutylicum* HPr (HPR_CAC) and putative Crh (CRH_CAC0149) with Crh proteins from several *Bacillus* species using the CLUSTALW (ver. 1.8) Multiple Sequence Alignment tool. CRH_BSU = *B. subtilis* Crh, CRH_BLI = *B. licheniformis* Crh, CRH_BHA = *B. halodurans* Crh, CRH_BCL = *B. clausii* Crh. The blue box highlights the conserved N-terminal histidine residue of HPr required for phosphotransfer to the PTS that is not present in the Crh proteins. The red box highlights the conserved C-terminal serine residue that when phosphorylated promotes activation of CCR through interaction with CcpA. (B) Fold expression of CA_C0149 in the indicated carbohydrate source relative to glucose expression in *C. acetobutylicum* obtained from a previous transcriptomic study (19).

is added, importers and enzymes converting arabinose to xylulose-5-P must be synthesized, causing a graded increase in arabinose uptake and utilization. We speculate that this gradual increase in arabinose import unintuitively leads to rapid growth since it avoids a sudden production of toxic intermediates.

Addition of glucose or arabinose reduced xylose utilization (Fig. 2B and C), thus confirming that the presence of arabinose in the medium inhibits xylose utilization via a mechanism that cannot entirely be due to a lower growth rate on xylose. Xylose utilization in the (+)Ara cultures resumed rapidly upon depletion of arabinose. In contrast, xylose utilization in the (+)Glu cultures took much longer to recover after glucose was depleted (Fig. 2B). The difference in the time of resumption of xylose utilization between the (+)Ara and (+)Glu is probably due to more metabolic machinery for xylose utilization being present in the (+)Ara cultures than in the (+)Glu cultures since arabinose and xylose are both metabolized via the PKP and PPP. These observations are consistent with a recent report showing that when cells are fed glucose-xylose mixtures, the xylose is utilized only to produce PPP intermediates for biosynthetic reactions (21). We cannot rule out the possibility that there are subpopulations that are

consuming different sugars, as this has been observed in other bacteria and may play a role in clostridia (31, 37, 38).

Recent publications show that arabinose favors carbon flux through the PKP compared to the PPP and that the reduced oxidation of carbon to CO₂ when the PKP is utilized results in an increase in acetate production (15–18). Xylose flux through the PKP is concentration dependent, and the concentrations of xylose used in this study were not expected to cause increased flux of xylose via the PKP (16, 18). This difference in metabolism is reflected in the arabinose-supplemented culture, which has significantly higher acetate production than any other condition, indicating that arabinose addition shifted carbon flux from the PPP to the PKP (Fig. 2D). This is consistent with a recent report by Aristilde et al., which showed high levels of flux through the PKP when cells were fed xylose-arabinose mixtures (17). The shift to PKP metabolism is further supported by increased expression of the *xfp* gene upon addition of arabinose, which was not seen under any of the other conditions (Fig. 4A). Final concentrations of acetate and butyrate in the (+)Glu and (+)Xyl cultures are similar, which was expected because molar equivalent amounts of carbon from glucose and xylose were converted to acetyl-CoA and CO₂ through the Embden-Meyerhof-Parnas (EMP) pathway and the PPP coupled to the EMP, respectively, resulting in nearly equivalent production of ATP and reduced electron carriers (15).

Expression of XylR- and AraR-controlled genes was severely reduced by 15 min after glucose addition and continued to drop through the hour (Fig. 4). These results were expected, since glucose-mediated CCR is well documented in *C. acetobutylicum*, and the presence of CRE sequences associated with AraR- and XylR-controlled genes is the likely mechanism for inhibition of xylose metabolism in the (+)Glu culture. Several genes, including the PKP gene *xfp* (CA_C1343), lack identified CRE sites but were repressed by glucose addition, indicating that these genes have unidentified CRE sites or some other form of regulation (Fig. 4A). CCR mediated by glucose metabolism is well understood, but it was not obvious how arabinose mediated repression of xylose utilization in these cultures.

Sample clustering indicated that as time progressed, gene expression in the (+)Ara and (+)Glu converged (Fig. 3A). There was a large overlap in the differentially expressed genes at the 60-min time point, and many of these genes have been shown to be CcpA controlled (Fig. 3B). The time delay between the glucose and arabinose responses is evident in Fig. 4C when comparing the yellow and orange lines for glucose and arabinose, respectively. The overlap between the samples indicated that arabinose was activating CCR mediated by CcpA and Crh via the model proposed in Fig. 6. The proposed model for arabinose activation of CCR is founded in the fact that in *C. acetobutylicum* arabinose metabolism is more rapid than xylose metabolism. An increased metabolic rate would result in more rapid flux to the EMP pathway via glyceraldehyde 3-phosphate (G3P), leading to higher fructose 1,6-bisphosphate (FBP) levels and activation of HPr kinase (39) (Fig. 6). The aldolase reaction that converts FBP into dihydroxyacetone phosphate (DHAP) and G3P has been shown to be highly reversible in *C. acetobutylicum*, indicating that an increase of G3P would increase FBP levels (40). The result would be phosphorylation of HPr and/or the putative Crh, subsequently leading to CcpA-mediated CCR. The delay in repression by arabinose relative to glucose was probably due to the need to produce CA_C1343 (*xfp*) in order to increase flux to the EMP pathway via the PKP. This is in contrast to the glucose utilization enzymes, which would have been present and immediately available to metabolize glucose, consequently increasing EMP pathway flux and resulting in CCR.

There have been very few Crh orthologues identified, and to our knowledge, the only one putatively identified in *Clostridium* is in *Clostridium cellulolyticum* (41). In the current and previous studies, transcript levels of the putative *C. acetobutylicum* Crh gene (CA_C0149) were increased during growth on less preferred carbohydrates (Fig. 5B). Active repression of CA_C0149 when preferred carbohydrates are added coupled with a putative CRE site upstream of CA_C0149 indicates that expression of the

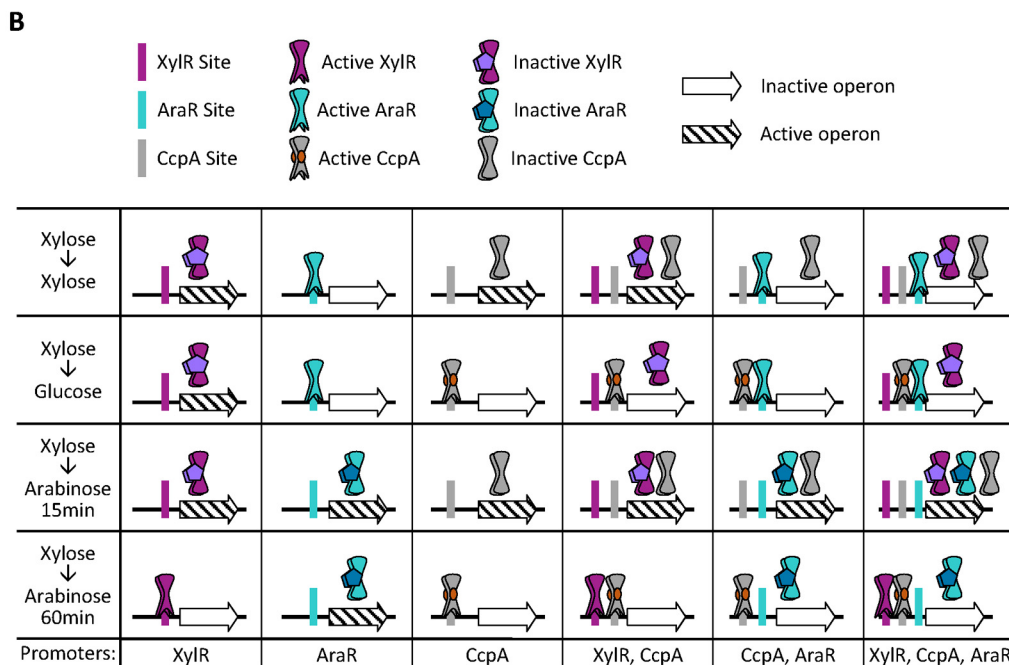
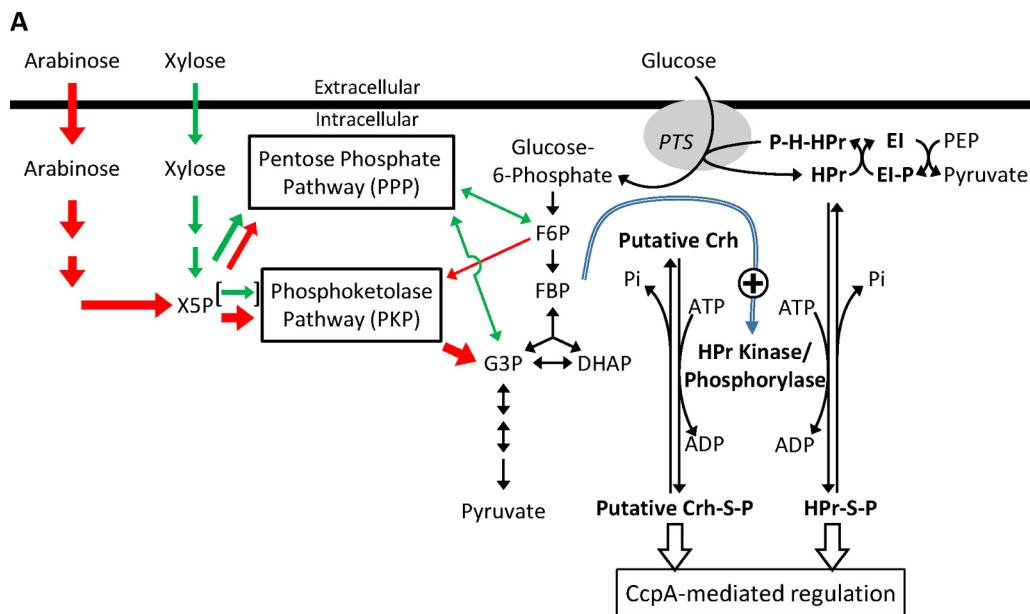


FIG 6 Proposed role of putative Crh and mechanism of catabolite repression by arabinose in *C. acetobutylicum*. (A) Schematic of central metabolic pathways and activation of CcpA-mediated CCR via phosphorylated HPr or Crh. Initial arabinose metabolic steps are shown in red, and xylose metabolic steps are shown in green. The increased metabolic rates during growth on arabinose compared to xylose are indicated by arrow thickness. Increased levels of FBP during growth on arabinose or glucose compared to xylose could activate HPrK, leading to phosphorylation of HPr and/or Crh. (B) Schematic showing interactions of repressor proteins during different nutritional states with genes having different regulatory schemes. Xylose to xylose: XylR binds xylose and XylR genes are derepressed, AraR is active and repressing AraR genes, CcpA is not active. Xylose to glucose: CcpA is activated, lack of intracellular arabinose and xylose causes repression via AraR and XylR. Xylose to arabinose 15 min: AraR binds arabinose resulting in derepression by AraR, XylR binds xylose, and XylR genes are derepressed, CcpA is not activated due to insufficient FBP levels to activate HPrK. Xylose to arabinose 60 min: AraR is derepressed due to arabinose binding, decreased import of xylose causes repression of XylR genes, and CcpA acts a repressor due to increased FBP levels as a result of increased metabolic rate following phosphoketolase activation.

gene is modulated by CcpA. The putative *C. acetobutylicum* Crh identified in this study needs further investigation to verify a regulatory role of the protein and determine if it interacts with HPr kinase and CcpA. Additionally, if Crh is involved with catabolite repression, the different roles for HPr and Crh require elucidation.

There is a possible second level of regulation for XylR-controlled genes. Addition of arabinose resulted in an increase in expression of both the PKP and PPP genes, likely due to the presence of AraR binding sites upstream of these operons/genes that enable transcription to proceed in the presence of arabinose. This would relieve any potential bottlenecks in xylose metabolism downstream of xylulose-5-P due to induction of the PKP, causing a drop in intracellular xylose concentrations. Decreased intracellular xylose concentration would alter the ratio of unbound to xylose-bound XylR repressor, which would promote XylR-mediated repression of the XylR-controlled gene. Reduction of intracellular xylose concentration could be further exacerbated if the predicted sugar/cation symporter CA_C1339 (*araE1*) transports both arabinose and xylose, as has been demonstrated for many bacterial pentose transporters, such as in *B. subtilis*, *E. coli*, and *Salmonella enterica* serovar Typhimurium (42, 43). Previous transcriptomic data suggested that CA_C1339 (*araE1*) was a xylose-specific transporter; however, bioinformatic analysis found an AraR binding site in its promoter region, implying a role in arabinose transport as well (19). The RNA-Seq data in this study showed that CA_C3451 (*xynT*) and CA_C1339 (*araE1*) are highly expressed in xylose-grown cultures; however, only CA_C1339 (*araE1*) has increased expression in response to arabinose, suggesting that it is involved in transport of xylose and arabinose. This expression pattern prompted us to investigate the CA_C1339 promoter region. Emboss matcher (44) identified a site 84 bases upstream of the transcription start site that has homology to sites identified upstream of XylR genes and overlaps the predicted SigA binding site in its promoter region, indicating that transcription of this predicted pentose transporter is controlled by both AraR and XylR (45). Promiscuous pentose transporters in other bacteria have been demonstrated to have a higher affinity and transport rate for arabinose than xylose. If also true in *C. acetobutylicum*, this could contribute to the preference for arabinose by creating a bottleneck for xylose import and requires further investigation.

It is unclear what the metabolic advantage is, if one exists, for the hierarchy of arabinose over xylose, but it is present among many lineages of bacteria and is mediated by a variety of regulatory schemes. One possible explanation is the relative availability of xylose and arabinose in the environment. While there is a higher ratio of xylose to arabinose in lignocellulosic biomass overall, the opposite is true for one of its components, pectin, a polysaccharide component found in primary cell walls (46). Clostridia are well known for their pectinolytic nature in the degradation of plant matter (47), and a selective advantage may exist for *C. acetobutylicum* to target the arabinose-rich pectin before utilizing the more recalcitrant secondary cell wall components. This strategy would be even more advantageous for consumption of the rapidly degraded pectin-rich plant matter found in plant-derived foods, such as fruits and vegetables (48).

The data presented here demonstrate that transcriptional regulation in *C. acetobutylicum* is a critical component of pentose hierarchy, and provide insight into the underpinning biochemical regulation through arabinose activation of CCR via a newly identified putative Crh. A deeper understanding of this regulation allows informed engineering of the organism and modulation of fermentation conditions to fine-tune desired chemical production from *C. acetobutylicum* grown on pentose-rich biomass. The ability to modulate metabolism via the PKP and PPP would provide a means to control carbon flow and the redox state of the cells so that they match the requirements for chemical synthesis via natural or engineered pathways. CA_C0149 may represent a potential control point for pentose and hexose utilization in *C. acetobutylicum* to allow full, simultaneous utilization of these abundant sugars in lignocellulosic biomass. Additionally, the RNA-Seq data provide information about genes that are potentially involved in pentose hierarchy mechanisms and will provide guidance for future studies.

MATERIALS AND METHODS

Bacterial strain and growth conditions. *Clostridium acetobutylicum* ATCC 824 was utilized for all studies. All growth was conducted anaerobically in a Coy anaerobic chamber (Coy Lab Products) at 37°C

in an atmosphere containing 5% H₂, 5% CO₂, and 90% N₂. Cells were maintained as spore suspensions in potato glucose medium (PGM) containing, per liter, 150 g potato (shredded, boiled 1 h, and filtered through cheesecloth), 1% glucose, 30 mM CaCO₃, and 4 mM (NH₄)₂SO₄ (49). Experimental cultures were grown in clostridium growth medium (CGM) containing, per liter, 0.5% yeast extract, 15 mM (NH₄)₂SO₄, 15 mM L-asparagine, 17 mM NaCl, 5 mM KH₂(PO₄), 3 mM Mg(SO₄)·H₂O, 0.7 mM Mn(SO₄)·H₂O, 0.4 mM Fe(SO₄)·7H₂O (50).

Experimental growth and sample collection. All cultures were incubated at 37°C under anaerobic conditions open to the environment of the anaerobe chamber, without shaking. Spores were heat shocked at 80°C for 10 min and inoculated into CGM supplemented with 0.5% xylose. Starter cultures were subcultured into 0.5% xylose CGM and incubated overnight. At an OD₆₀₀ of 0.2, the culture was aliquoted into milk dilution bottles (70 ml each; four conditions in three independent biological replicates) and incubated until the OD₆₀₀ reached 0.4. Precarbohydrate supplementation RNA and metabolite analysis samples were collected. Cultures were then supplemented with arabinose (0.25% final), glucose (0.25% final), or xylose (0.25% final), from a 50% stock solution of the respective sugars in water, or an equal volume of water (control). Separate samples for RNA, metabolites, and OD₆₀₀ readings were taken at 0 min (no RNA collected for this time point), 15 min, 30 min, and 60 min. Cultures were monitored for an additional 9 h, and metabolite samples and OD₆₀₀ readings were taken every hour. Final OD₆₀₀ readings and metabolite samples were taken the following day at 21 h after supplemental sugar addition. Samples collected for RNA isolation were immediately incubated with 0.03 mg/ml rifampin (final concentration) on ice, pelleted, treated with RNAprotect (Qiagen, Valencia, CA) according to the manufacturer's protocol, and stored at -80°C until RNA extraction. Metabolite samples were filter sterilized and stored at -20°C until analysis.

RNA extraction, purification, and rRNA depletion. Total RNA was isolated using the miRNeasy minikit (Qiagen; 217004) according to the manufacturer's protocol, with an additional homogenization and mechanical disruption step using a bead beater (BioSpec, Bartlesville, OK, USA) with zirconia-silica beads (BioSpec; 11079101z). RNA quality was assessed using the 2100 Bioanalyzer (Agilent Technologies, Santa Clara, CA, USA), RNA was quantified using a spectrophotometer (DeNovix, Wilmington, DE, USA), and it was stored at -80°C until DNase treatment. DNA was removed using the Turbo DNA-free kit (Life Technologies; AM1907) according to the manufacturer's protocol. RNA was quantified and quality assessed, as stated above, and genomic DNA depletion was confirmed using quantitative PCR (qPCR) with 16S rRNA gene primers (19) and iQ SYBR Green Supermix (Bio-Rad; 170-8882) according to the manufacturer's instructions. rRNA was removed using the Ribo-Zero rRNA removal kit (Gram-positive bacteria) (Illumina; MRZGP126) according to the manufacturer's protocol. The quality of rRNA-depleted samples was assessed using a 2100 Bioanalyzer prior to processing for sequencing library generation.

Sequencing library preparation. The TruSeq stranded mRNA sample preparation kit (Illumina; RS-122-2101) was used to prepare the rRNA-depleted RNA for sequencing according to the manufacturer's protocol with the adaptations suggested for purified mRNA input. Libraries were quantified using the Kapa library quantification kit (Kapa Biosystems; KK4854) according to the manufacturer's instructions and then normalized and pooled for sequencing according to the Denature and Dilute Libraries Guide for the NextSeq 500 (Illumina; document no. 15048776 v02). Pooled libraries were 1- by 75-bp sequenced on a NextSeq 500 (Illumina, San Diego, CA, USA) in two sequencing runs.

RNA-Seq data analysis. Samples had an average of 14 million reads each, were assessed for quality using FastQC, and were trimmed to remove Illumina adaptors and low-quality bases using Trimmomatic (51, 52). Samples were mapped to the *Clostridium acetobutylicum* ATCC 824 reference genome (GenBank accession numbers [AE001437.1](#) and [AE001438.3](#)) using EDGE-pro (53), and differential gene expression was evaluated using DESeq2 with default parameters (54). (+)Ara, (+)Glu, and (+)Xyl were compared to (+)None at matching time points after supplemental sugar addition and analyzed for differential gene expression. For validation, the same comparisons were assessed for differential gene comparison and operon prediction using Rockhopper (55), and there was good agreement between the two pipelines. Genes that met a *P* value cutoff of 0.05 and a fold change cutoff of 4 were considered to have differential expression.

Statistical analysis. To focus on highly expressed genes, we filtered genes that had an RPKM greater than the overall third quartile RPKM value in at least one sample. We also removed putative phage Clo1 (CA_C1113-1197) and Clo2 (CA_C1878-1957) genes from the analysis (24). R v 3.2.3 (56) was used for all analyses, and plots were generated with ggplot2 (57). Venn diagrams were generated with the VennDiagram package (58). Heat maps were generated with the heatmaply package using hierarchical clustering of Euclidean distances (59). We assigned transcriptional regulation sites (AraR and XylR) according to RegPrecise (60) predictions and included all downstream genes in operons (according to DOOR [61-63] predictions). We also included CcpA site predictions from the work of Ren et al. in addition to the genes that had differential expression after *ccpA* inactivation (23).

Metabolite analysis. High-performance liquid chromatography (HPLC) analysis of external metabolites (carbohydrates, acetate, butyrate, acetone, butanol, and ethanol) was performed on an Agilent 1200 equipped with a refractive index detector using an Aminex HPX-87H cation exchange column (300 mm by 7.8 mm inside diameter [i.d.] by 9 μm) from Bio-Rad Laboratories. Samples (20 μl) were injected into the HPLC system and eluted isocratically with a mobile phase of 3.25 mM H₂SO₄ at 0.6 ml/min and 65°C. Quantification was based on an external calibration curve using pure known components as standards (64).

Data availability. The raw RNA-Seq data sets and gene expression tables generated during this study are available through NCBI's GEO database (accession no. [GSE107804](#)).

SUPPLEMENTAL MATERIAL

Supplemental material for this article may be found at <https://doi.org/10.1128/mSystems.00064-18>.

FIG S1, TIF file, 1 MB.

REFERENCES

- Wells CL, Wilkins TD. 1996. Clostridia: sporeforming anaerobic bacilli. In Baron S (ed), Medical microbiology, 4th ed. University of Texas Medical Branch at Galveston, Galveston, TX.
- Pfromm PH, Amanor-Boadu V, Nelson R, Vadlani P, Madl R. 2010. Bio-butanol vs. bio-ethanol: a technical and economic assessment for corn and switchgrass fermented by yeast or *Clostridium acetobutylicum*. *Biomass Bioenergy* 34:515–524. <https://doi.org/10.1016/j.biombioe.2009.12.017>.
- Awang GM, Jones GA, Ingledew WM. 1988. The acetone-butanol-ethanol fermentation. *Crit Rev Microbiol* 15:533–567. <https://doi.org/10.3109/10408418809104464>.
- Ho DP, Ngo HH, Guo W. 2014. A mini review on renewable sources for biofuel. *Bioresour Technol* 169:742–749. <https://doi.org/10.1016/j.biortech.2014.07.022>.
- Ezeji T, Blaschek HP. 2008. Fermentation of dried distillers' grains and solubles (DDGS) hydrolysates to solvents and value-added products by solventogenic clostridia. *Bioresour Technol* 99:5232–5242. <https://doi.org/10.1016/j.biortech.2007.09.032>.
- Saha BC, Iten LB, Cotta MA, Wu YV. 2005. Dilute acid pretreatment, enzymatic saccharification and fermentation of wheat straw to ethanol. *Process Biochem* 40:3693–3700. <https://doi.org/10.1016/j.procbio.2005.04.006>.
- Xiao H, Gu Y, Ning Y, Yang Y, Mitchell WJ, Jiang W, Yang S. 2011. Confirmation and elimination of xylose metabolism bottlenecks in glucose phosphoenolpyruvate-dependent phosphotransferase system-deficient *Clostridium acetobutylicum* for simultaneous utilization of glucose, xylose, and arabinose. *Appl Environ Microbiol* 77:7886–7895. <https://doi.org/10.1128/AEM.00644-11>.
- El Kanouni A, Zerdani I, Zaafa S, Znassni M, Loutfi M, Boudouma M. 1998. The improvement of glucose/xylose fermentation by *Clostridium acetobutylicum* using calcium carbonate. *World J Microbiol Biotechnol* 14: 431–435. <https://doi.org/10.1023/A:1008881731894>.
- Zhang L, Leyn SA, Gu Y, Jiang W, Rodionov DA, Yang C. 2012. Ribulokinase and transcriptional regulation of arabinose metabolism in *Clostridium acetobutylicum*. *J Bacteriol* 194:1055–1064. <https://doi.org/10.1128/JB.06241-11>.
- Gu Y, Ding Y, Ren C, Sun Z, Rodionov DA, Zhang WW, Yang S, Yang C, Jiang WH. 2010. Reconstruction of xylose utilization pathway and regulons in Firmicutes. *BMC Genomics* 11:255. <https://doi.org/10.1186/1471-2164-11-255>.
- Procentese A, Raganati F, Olivieri G, Russo ME, Salatino P, Marzocchella A. 2014. Continuous xylose fermentation by *Clostridium acetobutylicum*—kinetics and energetics issues under acidogenesis conditions. *Bioresour Technol* 164:155–161. <https://doi.org/10.1016/j.biortech.2014.04.054>.
- Procentese A, Raganati F, Olivieri G, Russo ME, Salatino P, Marzocchella A. 2015. Continuous xylose fermentation by *Clostridium acetobutylicum*—assessment of solventogenic kinetics. *Bioresour Technol* 192: 142–148. <https://doi.org/10.1016/j.biortech.2015.05.041>.
- Bruder M, Moo-Young M, Chung DA, Chou CP. 2015. Elimination of carbon catabolite repression in *Clostridium acetobutylicum*—a journey toward simultaneous use of xylose and glucose. *Appl Microbiol Biotechnol* 99:7579–7588. <https://doi.org/10.1007/s00253-015-6611-4>.
- Grimmler C, Held C, Liebl W, Ehrenreich A. 2010. Transcriptional analysis of catabolite repression in *Clostridium acetobutylicum* growing on mixtures of D-glucose and D-xylose. *J Biotechnol* 150:315–323. <https://doi.org/10.1016/j.jbiotec.2010.09.938>.
- Servinsky MD, Germane KL, Liu S, Kiel JT, Clark AM, Shankar J, Sund CJ. 2012. Arabinose is metabolized via a phosphoketolase pathway in *Clostridium acetobutylicum* ATCC 824. *J Ind Microbiol Biotechnol* 39: 1859–1867. <https://doi.org/10.1007/s10295-012-1186-x>.
- Liu L, Zhang L, Tang W, Gu Y, Hua Q, Yang S, Jiang W, Yang C. 2012. Phosphoketolase pathway for xylose catabolism in *Clostridium acetobutylicum* revealed by ¹³C metabolic flux analysis. *J Bacteriol* 194: 5413–5422. <https://doi.org/10.1128/JB.00713-12>.
- Aristilde L, Lewis IA, Park JO, Rabinowitz JD. 2015. Hierarchy in pentose sugar metabolism in *Clostridium acetobutylicum*. *Appl Environ Microbiol* 81:1452–1462. <https://doi.org/10.1128/AEM.03199-14>.
- Sund CJ, Liu S, Germane KL, Servinsky MD, Gerlach ES, Hurley MM. 2015. Phosphoketolase flux in *Clostridium acetobutylicum* during growth on L-arabinose. *Microbiology* 161:430–440. <https://doi.org/10.1099/mic.0.000008>.
- Servinsky MD, Kiel JT, Dupuy NF, Sund CJ. 2010. Transcriptional analysis of differential carbohydrate utilization by *Clostridium acetobutylicum*. *Microbiology* 156:3478–3491. <https://doi.org/10.1099/mic.0.037085-0>.
- Tangney M, Galinier A, Deutscher J, Mitchell WJ. 2003. Analysis of the elements of catabolite repression in *Clostridium acetobutylicum* ATCC 824. *J Mol Microbiol Biotechnol* 6:6–11. <https://doi.org/10.1159/000073403>.
- Aristilde L. 2017. Metabolite labelling reveals hierarchies in *Clostridium acetobutylicum* that selectively channel carbons from sugar mixtures towards biofuel precursors. *Microb Biotechnol* 10:162–174. <https://doi.org/10.1111/1751-7915.12459>.
- Gorke B, Stulke J. 2008. Carbon catabolite repression in bacteria: many ways to make the most out of nutrients. *Nat Rev Microbiol* 6:613–624. <https://doi.org/10.1038/nrmicro1932>.
- Ren C, Gu Y, Wu Y, Zhang W, Yang C, Yang S, Jiang W. 2012. Pleiotropic functions of catabolite control protein CcpA in butanol-producing *Clostridium acetobutylicum*. *BMC Genomics* 13:349. <https://doi.org/10.1186/1471-2164-13-349>.
- Nolling J, Breton G, Omelchenko MV, Makarova KS, Zeng Q, Gibson R, Lee HM, Dubois J, Qiu D, Hitti J, Wolf YI, Tatusov RL, Sabathe F, Doucette-Stamm L, Soucaille P, Daly MJ, Bennett GN, Koonin EV, Smith DR. 2001. Genome sequence and comparative analysis of the solvent-producing bacterium *Clostridium acetobutylicum*. *J Bacteriol* 183:4823–4838. <https://doi.org/10.1128/JB.183.16.4823-4838.2001>.
- Martin-Verstraete I, Deutscher J, Galinier A. 1999. Phosphorylation of HPr and Crh by HPrK, early steps in the catabolite repression signalling pathway for the *Bacillus subtilis* levanase operon. *J Bacteriol* 181:2966.
- Galiner A, Haiech J, Kilhoffer MC, Jaquinod M, Stulke J, Deutscher J, Martin-Verstraete I. 1997. The *Bacillus subtilis* crh gene encodes a HPr-like protein involved in carbon catabolite repression. *Proc Natl Acad Sci U S A* 94:8439–8444. <https://doi.org/10.1073/pnas.94.16.8439>.
- Warner JB, Lolkema JS. 2003. CcpA-dependent carbon catabolite repression in bacteria. *Microbiol Mol Biol Rev* 67:475–490. <https://doi.org/10.1128/MMBR.67.4.475-490.2003>.
- Rodionov DA, Mironov AA, Gelfand MS. 2001. Transcriptional regulation of pentose utilisation systems in the *Bacillus/Clostridium* group of bacteria. *FEMS Microbiol Lett* 205:305–314. <https://doi.org/10.1111/j.1574-6968.2001.tb10965.x>.
- Mitchell WJ. 2015. The phosphotransferase system in solventogenic clostridia. *J Mol Microbiol Biotechnol* 25:129–142. <https://doi.org/10.1159/000375125>.
- Hu S, Zheng H, Gu Y, Zhao J, Zhang W, Yang Y, Wang S, Zhao G, Yang S, Jiang W. 2011. Comparative genomic and transcriptomic analysis revealed genetic characteristics related to solvent formation and xylose utilization in *Clostridium acetobutylicum* EA 2018. *BMC Genomics* 12:93. <https://doi.org/10.1186/1471-2164-12-93>.
- Koirala S, Wang X, Rao CV. 2016. Reciprocal regulation of L-arabinose and D-xylose metabolism in *Escherichia coli*. *J Bacteriol* 198:386–393. <https://doi.org/10.1128/JB.00709-15>.
- Desai TA, Rao CV. 2010. Regulation of arabinose and xylose metabolism in *Escherichia coli*. *Appl Environ Microbiol* 76:1524–1532. <https://doi.org/10.1128/AEM.01970-09>.
- Kang HY, Song S, Park C. 1998. Priority of pentose utilization at the level of transcription: arabinose, xylose, and ribose operons. *Mol Cells* 8:318–323.

34. Aidelberg G, Towbin BD, Rothschild D, Dekel E, Bren A, Alon U. 2014. Hierarchy of non-glucose sugars in *Escherichia coli*. *BMC Syst Biol* 8:133. <https://doi.org/10.1186/s12918-014-0133-z>.
35. Landmann JJ, Busse RA, Latz JH, Singh KD, Stulke J, Gorke B. 2011. Crh, the paralogue of the phosphocarrier protein HPr, controls the methylglyoxal bypass of glycolysis in *Bacillus subtilis*. *Mol Microbiol* 82:770–787. <https://doi.org/10.1111/j.1365-2958.2011.07857.x>.
36. Kadner RJ, Murphy GP, Stephens CM. 1992. Two mechanisms for growth inhibition by elevated transport of sugar phosphates in *Escherichia coli*. *J Gen Microbiol* 138:2007–2014. <https://doi.org/10.1099/0021287-138-10-2007>.
37. Beisel CL, Afroz T. 2016. Rethinking the hierarchy of sugar utilization in bacteria. *J Bacteriol* 198:374–376. <https://doi.org/10.1128/JB.00890-15>.
38. Kolek J, Branska B, Drahokoupil M, Patakova P, Melzoch K. 2016. Evaluation of viability, metabolic activity and spore quantity in clostridial cultures during ABE fermentation. *FEMS Microbiol Lett* 363:fnw031. <https://doi.org/10.1093/femsle/fnw031>.
39. Reizer J, Hoischen C, Titgemeyer F, Rivolta C, Rabus R, Stulke J, Karamata D, Saier MH, Jr, Hillen W. 1998. A novel protein kinase that controls carbon catabolite repression in bacteria. *Mol Microbiol* 27:1157–1169. <https://doi.org/10.1046/j.1365-2958.1998.00747.x>.
40. Rabinowitz J, Aristilde L, Amador-Noguez D. 2015. Metabolomics of clostridial biofuel production. United States Department of Energy, Washington, DC.
41. Abdou L, Boileau C, de Philip P, Pages S, Fierobe HP, Tardif C. 2008. Transcriptional regulation of the *Clostridium cellulolyticum* *cip-cel* operon: a complex mechanism involving a catabolite-responsive element. *J Bacteriol* 190:1499–1506. <https://doi.org/10.1128/JB.01160-07>.
42. Krispin O, Allmansberger R. 1998. The *Bacillus subtilis* AraE protein displays a broad substrate specificity for several different sugars. *J Bacteriol* 180:3250–3252.
43. Novotny CP, Englesberg E. 1966. The L-arabinose permease system in *Escherichia coli* B/r. *Biochim Biophys Acta* 117:217–230. [https://doi.org/10.1016/0304-4165\(66\)90169-3](https://doi.org/10.1016/0304-4165(66)90169-3).
44. Rice P, Longden I, Bleasby A. 2000. EMBOSS: the European molecular biology open software suite. *Trends Genet* 16:276–277. [https://doi.org/10.1016/S0168-9525\(00\)02024-2](https://doi.org/10.1016/S0168-9525(00)02024-2).
45. Paredes CJ, Rigoutsos I, Papoutsakis ET. 2004. Transcriptional organization of the *Clostridium acetobutylicum* genome. *Nucleic Acids Res* 32:1973–1981. <https://doi.org/10.1093/nar/gkh509>.
46. Xiao C, Anderson CT. 2013. Roles of pectin in biomass yield and processing for biofuels. *Front Plant Sci* 4:67. <https://doi.org/10.3389/fpls.2013.00067>.
47. Schink B, Ward J, Zeikus G. 1981. Microbiology of wetwood: importance of pectin degradation and *Clostridium* species in living trees. *Appl Environ Microbiol* 42:526–532.
48. Muller-Maatsch J, Bencivenni M, Caligiani A, Tedeschi T, Bruggeman G, Bosch M, Petrusan J, Van Droogenbroeck B, Elst K, Sforza S. 2016. Pectin content and composition from different food waste streams. *Food Chem* 201:37–45. <https://doi.org/10.1016/j.foodchem.2016.01.012>.
49. Al-Shorgani NKN, Tibin E-M, Ali E, Hamid AA, Yusoff WMW, Kalil MS. 2014. Biohydrogen production from agroindustrial wastes via *Clostridium saccharoperbutylacetonicum* N1-4 (ATCC 13564). *Clean Technol Environ Policy* 16:11–21. <https://doi.org/10.1007/s10098-013-0586-6>.
50. Servinsky MD, Liu S, Gerlach ES, Germane KL, Sund CJ. 2014. Fermentation of oxidized hexose derivatives by *Clostridium acetobutylicum*. *Microb Cell Fact* 13:139. <https://doi.org/10.1186/s12934-014-0139-7>.
51. Bolger AM, Lohse M, Usadel B. 2014. Trimmomatic: a flexible trimmer for Illumina sequence data. *Bioinformatics* 30:2114–2120. <https://doi.org/10.1093/bioinformatics/btu170>.
52. Andrews S. 2010. FastQC: a quality control tool for high throughput sequence data. www.bioinformatics.babraham.ac.uk/projects/fastqc.
53. Magoc T, Wood D, Salzberg SL. 2013. EDGE-pro: estimated degree of gene expression in prokaryotic genomes. *Evol Bioinform Online* 9:127–136.
54. Love MI, Huber W, Anders S. 2014. Moderated estimation of fold change and dispersion for RNA-seq data with DESeq2. *Genome Biol* 15:550. <https://doi.org/10.1186/s13059-014-0550-8>.
55. Tjaden B. 2015. *De novo* assembly of bacterial transcriptomes from RNA-seq data. *Genome Biol* 16:1. <https://doi.org/10.1186/s13059-014-0572-2>.
56. R Core Team. 2015. R: a language and environment for statistical computing. R Foundation for Statistical Computing, Vienna, Austria. www.R-project.org/.
57. Wickham H. 2009. ggplot2: elegant graphics for data analysis. Springer-Verlag, New York, NY.
58. Chen H. 2016. VennDiagram: generate high-resolution Venn and Euler plots. <https://cran.r-project.org/web/packages/VennDiagram/index.html>.
59. Galili T, Sidi J, O'Callaghan A, Benjamini Y. 2017. heatmaply: interactive cluster heat maps using 'plotly'. <https://cran.r-project.org/web/packages/heatmaply/index.html>.
60. Novichkov PS, Kazakov AE, Ravcheev DA, Leyn SA, Kovaleva GY, Surtornin RA, Kazanov MD, Riehl W, Arkin AP, Dubchak I, Rodionov DA. 2013. RegPrecise 3.0—a resource for genome-scale exploration of transcriptional regulation in bacteria. *BMC Genomics* 14:745. <https://doi.org/10.1186/1471-2164-14-745>.
61. Mao F, Dam P, Chou J, Olman V, Xu Y. 2009. DOOR: a database for prokaryotic operons. *Nucleic Acids Res* 37:D459–D463. <https://doi.org/10.1093/nar/gkn757>.
62. Mao XZ, Ma Q, Zhou C, Chen X, Zhang HY, Yang JC, Mao FL, Lai W, Xu Y. 2014. DOOR 2.0: presenting operons and their functions through dynamic and integrated views. *Nucleic Acids Res* 42:D654–D659. <https://doi.org/10.1093/nar/gkt1048>.
63. Dam P, Olman V, Harris K, Su Z, Xu Y. 2007. Operon prediction using both genome-specific and general genomic information. *Nucleic Acids Res* 35:288–298. <https://doi.org/10.1093/nar/gkl1018>.
64. Finch AS, Mackie TD, Sund CJ, Sumner JJ. 2011. Metabolite analysis of *Clostridium acetobutylicum*: fermentation in a microbial fuel cell. *Bioreour Technol* 102:312–315. <https://doi.org/10.1016/j.biortech.2010.06.149>.